Gate Control of Spin-Orbit Interaction in an Inverted $In_{0.53}Ga_{0.47}As/In_{0.52}Al_{0.48}As$ Heterostructure

Junsaku Nitta, Tatsushi Akazaki, and Hideaki Takayanagi
NTT Basic Research Laboratories, 3-1 Wakamiya, Morinosato, Atsugi-shi, Kanagawa 243-01, Japan

Takatomo Enoki
NTT System Electronics Laboratories, 3-1 Wakamiya, Morinosato, Atsugi-shi, Kanagawa 243-01, Japan
(Received 23 July 1996)

We have confirmed that a spin-orbit interaction in an inverted $In_{0.53}Ga_{0.47}As/In_{0.52}Al_{0.48}As$ quantum well can be controlled by applying a gate voltage. This result shows that the spin-orbit interaction of a two-dimensional electron gas depends on the surface electric field. The dominant mechanism for the change in the spin-orbit interaction parameter can be attributed to the Rashba term. This inverted $In_{0.53}Ga_{0.47}As/In_{0.52}Al_{0.48}As$ heterostructure is one of the promising materials for the spin-polarized field effect transistor which is proposed by Datta and Das [Appl. Phys. Lett. **56**, 665 (1990)]. [S0031-9007(97)02425-3]

PACS numbers: 73.20.Dx, 71.70.Ej, 75.25.+z

The concept of a spin-polarized field effect transistor has been proposed by Datta and Das [1]. The spin-polarized carriers are injected and collected by the ferromagnetic electrodes. The key idea of the above device is that a spin-orbit interaction in a narrow gap semiconductor quantum well causes the spins of the carriers to precess. The modulation of current can be expected by controlling the alignment of a carrier's spin with respect to the magnetization vector in the collector electrode. The gate electrode on the top of the device can be used for controlling the spin-orbit interaction if the spin-orbit interaction is dependent on the interface electric field. One of the unknown problems is to what extent the spin-orbit interaction can be controlled by the gate voltage.

Even without any external magnetic field, an electric field perpendicular to the two-dimensional electron gas (2DEG) yields an effective magnetic field for moving electrons which lifts the spin degeneracy. Two alternative mechanisms for spin splitting are important: (i) the host crystal electric field [2–5] and (ii) the interface electric field, the so-called Rashba mechanism [6,7]. Lommer *et al.* have pointed out that the Rashba mechanism becomes dominant in a narrow gap semiconductor system [8]. Luo *et al.* have experimentally shown that the Rashba term is dominant for spin splitting in an InAs based heterostructure [9]. Das and Datta *et al.* has obtained the spin splitting in three different $In_xGa_{1-x}As/In_{0.52}Al_{0.48}As$ systems from the beat pattern of Shubnikov–de Haas (SdH) oscillations [10]. The origin for this spin splitting in $In_xGa_{1-x}As/In_{0.52}Al_{0.48}As$ systems is believed to be the Rashba mechanism. The spin-splitting energy of 2DEG in an InAs/AlSb quantum well had been obtained as a function of the gate voltage by Heida *et al.* [11]. The spin-splitting energy Δ_R linearly increased by applying positive gate voltage. However, the origin for the increase in the spin-splitting energy has been attributed to the increase in the Fermi wave number k_F. Thus, the spin-orbit interaction parameter α, which is given by the relation $\Delta_R = 2k_F\alpha$, did not change significantly by applying a gate voltage. From the viewpoint of the proposed device, the most important parameter which governs the spin precession is the spin-orbit interaction parameter α. The spin-orbit interaction parameter is proportional to the expectation value of the electric field at the interface and, in principle, can be controlled by the applied gate voltage. However, this has not yet been demonstrated experimentally.

In this paper, the spin-orbit interaction in an inverted $In_{0.53}Ga_{0.47}As/In_{0.52}Al_{0.48}As$ heterostructure with a gate-fitted structure is studied for various electron concentrations by changing the gate voltage. The inverted-type heterostructure has a high breakdown voltage and a low gate-leakage current [12]. The spin-orbit interaction parameter has been obtained from the analysis of the beating pattern in the SdH oscillations. We have verified that the spin-orbit interaction parameter can be controlled by the gate voltage. The dominant mechanism for the change in the spin-orbit interaction parameter can be attributed to the Rashba term.

Figure 1 shows the layer structure of the inverted $In_{0.53}Ga_{0.47}As/In_{0.52}Al_{0.48}As$ modulation doped structure. The heterostructure used in this study was grown by molecular beam epitaxy (MBE) on a Fe-doped semi-insulating (100) InP substrate. All InGaAs and InAlAs layers were lattice matched to InP. The doping density of the 7-nm-thick $In_{0.52}Al_{0.48}As$ carrier supply layer which is underneath a 2DEG channel was 4×10^{18} cm^{-3}. The 2DEG channel was formed in an undoped $In_{0.53}Ga_{0.47}As$ channel layer of 20-nm thickness. The channel layer is separated by an undoped $In_{0.52}Al_{0.48}As$ spacer layer of 6-nm thickness to reduce ionized donor scattering.

A regular Hall bar sample was made with the above heterostructure. The gate electrode was made on the top of the 100-nm-thick SiO_2 insulating layer which covers

 © 1997 The American Physical Society

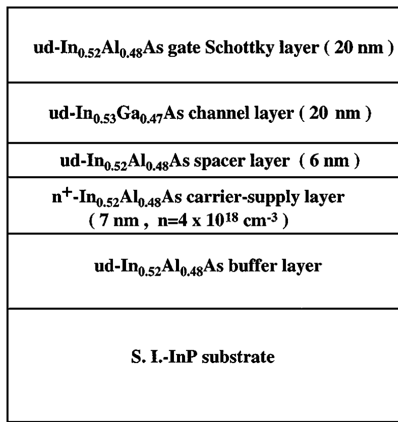

FIG. 1. Schematic layer structure of an inverted $In_{0.53}Ga_{0.47}As/In_{0.52}Al_{0.48}As$ heterostructure.

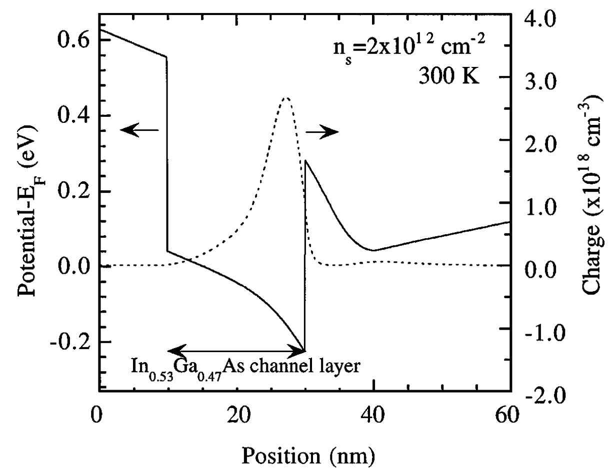

FIG. 2. Calculated conduction band diagram and electron distribution.

the Hall bar. The sample without a SiO_2 insulating layer and gate electrode was initially characterized by SdH measurement and its temperature dependence. The carrier concentration n_s was estimated to be 1.9×10^{12} cm^{-2} from the period of SdH. The fact that the different samples showed identical SdH patterns ensures the sample homogeneity. An electron mobility of 36 500 cm^2/Vs was obtained using the relation of $\mu = 1/\rho_{xx} n_s e$, where ρ_{xx} is sheet resistivity. From the temperature dependence of the SdH oscillation amplitude, the effective mass m^* of the electron was deduced to be $0.05 m_0$, where m_0 is the free electron mass. The gate voltage dependent carrier concentration was obtained from the period of SdH oscillation. The variations of Fermi energy and effective mass as a function of the gate voltage will be estimated below.

The calculated conduction band profile and 2DEG distribution of this heterostructure are shown in Fig. 2. The conduction band diagram is not symmetric although the $In_{0.53}Ga_{0.47}As$ channel layers is supported by the same $In_{0.52}Al_{0.48}As$ layers. The 2DEG distribution, which is shown by the dotted line, is located on the bottom side of the quantum well, close to the carrier supply layer. This asymmetry yields a surface electric field perpendicular to the 2DEG channel. The spin-orbit interaction parameter α is linearly dependent on the expectation value of the electric field $\langle E \rangle$ at 2DEG. This is given by

$$\alpha = b\langle E \rangle . \quad (1)$$

Here the coefficient b is inversely proportional to the energy gap and the effective mass [8]. By applying the negative gate voltage, the pinning potential at the interface between the $In_{0.52}Al_{0.48}As$ Schottky layer and the gate insulator will be shifted to a higher potential position. Thus the negative gate voltage will increase the potential gradient $\langle E \rangle$ which enhances α if the Rashba mechanism is dominant. It should be possible to distinguish which mechanism is dominant in this system from the gate voltage dependence, the host crystal field, or the interface electric field.

Figure 3 shows the gate voltage dependence of SdH oscillations at 0.4 K. The magnetic field B was applied perpendicular to the 2DEG. During the measurement, the applied electric field was carefully kept to be less than 1 V/m to avoid excess electron heating. Beat patterns are observed in the SdH oscillations because of the existence of two closely spaced SdH oscillation frequency components with similar amplitudes. These observed beat patterns can be attributed to the spin splitting. By increasing the positive gate voltage from $V_g = 0$ V to $V_g = 0.3$ V, the beat pattern became clear. Above $Vg = 0.5$ V, a clearly different low SdH oscillation frequency component becomes visible due to the occupation of the second subband. By making Vg more negative, oscillation frequency becomes lower because of the decrease in the carrier concentration. The second node position becomes unclear as Vg is decreased. One of the reasons is because the decrease in electron mobility causes the broadening of

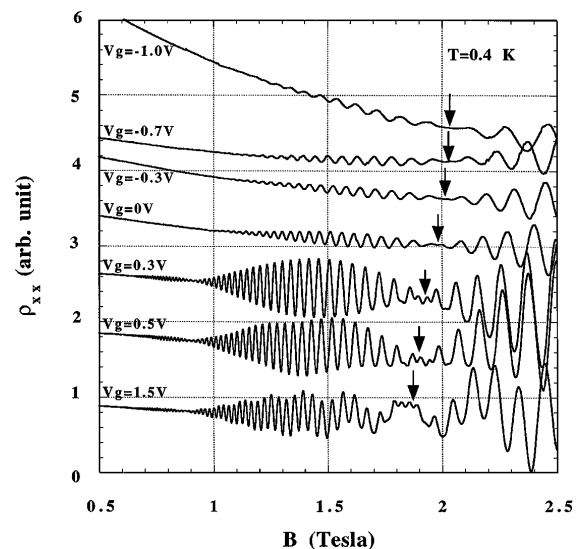

FIG. 3. Schubnikov–de Haas oscillations as a function of the gate voltages.

Landau levels. The first node position of the beat pattern is marked by an arrow in Fig. 3. The first node position shifts to a higher magnetic field as Vg is decreased. From $Vg = 1.5$ V to $Vg = 0.3$ V, the second node position also shifted to a higher magnetic field. It was also observed that the number of oscillations between the beat nodes decreases from $Vg = 1.5$ V to $Vg = 0.3$ V. These results suggest the increase in the spin-splitting energy.

The number of oscillations N between two nodes are $\sim$32–31 at $Vg = 1.5$ V and $\sim$27–26 at $Vg = 0.3$ V, respectively. The spin-splitting energy Δ is inversely proportional to the number of oscillations between the two nodes when the total number of electrons is held constant. The oscillation frequency reflects the electron carrier concentration. The carrier concentration decreased from 2.41×10^{12} cm^{-2} at $Vg = 1.5$ V to 2.23×10^{12} cm^{-2} at $Vg = 0.3$ V. If the change in the carrier concentration is taken into account, the ratio of the spin-splitting energy is approximately described by

$$\Delta_{Vg=0.3\ \mathrm{V}}/\Delta_{Vg=1.5\ \mathrm{V}} \sim N_{Vg=1.5\ \mathrm{V}} n_{sVg=0.3\ \mathrm{V}}/ N_{Vg=0.3\ \mathrm{V}} n_{sVg=1.5\ \mathrm{V}} \sim 1.1\,. \tag{2}$$

This result shows that the spin-splitting energy can be increased by applying a more negative gate voltage. The increase in the spin-splitting energy can be attributed to the surface electric field. At the same time, the negative gate voltage decreases the carrier concentration and therefore decreases the Fermi wave number k_F. These results lead to the increase in the spin-orbit interaction parameter α, and suggest that the Rashba mechanism is dominant.

To deduce the spin-orbit interaction parameter α, numerical calculation was performed to simulate the measured SdH oscillations. We followed the established method by Luo *et al.* [9] with the assumption that the origin for the spin splitting is the Rashba mechanism. The magnetoconductance of a 2DEG at $T = 0$ K is given by

$$\sigma_{xx} \propto \sum_{n\pm} (n \pm 1/2) \exp\left(-\frac{(E_F - E_n^{\pm})^2}{\Gamma^2}\right), \tag{3}$$

where E_F is the Fermi energy and E_n^{+} is the energy of the nth Landau level with spin up (+) and spin down (−). Here the Landau level broadening Γ is assumed to be a constant. In a magnetic field B, the energy spectrum for the nth Landau level is described by

$$E_0 = \frac{1}{2}\hbar\omega_c \qquad \text{when } n = 0,$$

$$E_n^{\pm} = \hbar\omega_c\left[n \pm \frac{1}{2}\sqrt{(1 - gm^*/2)^2 + n\frac{\Delta_R^2}{E_F\hbar\omega_c}}\right], \tag{4}$$

where ω_c is the cyclotron frequency which is given by $\omega_c = eB/m^*$, and g is the effective g factor. Here, it should be noted that in the Rashba model the spin-orbit interaction parameter α is the only variable, and the spin splitting does not appear in the calculation. However, we inserted the spin-splitting energy into Eq. (4) by using the relation $\Delta_R = 2k_F\alpha$. For quantizing magnetic fields ($\sigma_{xy} \gg \sigma_{xx}$), transverse resistivity ρ_{xx} is given as

$$\rho_{xx} = \sigma_{xx}/(\sigma_{xx}^2 + \sigma_{xy}^2) \approx \sigma_{xx}/\sigma_{xy}^2 \approx \sigma_{xx}(B/en_s)^2. \tag{5}$$

These equations clearly show a maximum in ρ_{xx} each time a Landau level passes through the Fermi energy, and a minimum when the Fermi energy is situated between two Landau levels.

The gate voltage dependent Fermi energy was obtained using n_s which is estimated from the SdH oscillation period. By applying a gate voltage from $Vg = +1.5$ V to -1.0 V, the carrier concentration n_s of the first subband was changed from 2.4×10^{12} to 1.6×10^{12} cm^{-2}. The energy dependence of effective mass m^* in the inverted $In_{0.53}Ga_{0.47}As/In_{0.52}Al_{0.48}As$ heterostructures was calculated in the previous report [13], and this calculation explained the experimentally obtained m^*. We used this relation to estimate the effective mass [13]. The variations of Fermi energy and effective mass in this gate voltage range were from 111 to 79 meV and from $0.052m_0$ to $0.049m_0$, respectively. The g factor was assumed to be 4 in these calculations. It should be noted that the g factor does not strongly affect the numerical simulation when it is less than 8.

Figure 4 compares the measured SdH oscillations and the numerical simulations. Here the values Δ_R and Γ were adjusted to fit the first node position of the beat pattern and to minimize the deviation between the experimental data and the calculations. At $Vg = -0.3$ V, the measured data can be well explained by the numerical simulation with $\Delta_R = 5.6$ meV and $\Gamma = 2.3$ meV. At $Vg = 0.3$ V, the oscillation above 2 T and the first node position can be well explained by the simulation with $\Delta_R = 5.2$ meV and $\Gamma = 1.4$ meV. The fact that the numerical simulations agree with the measured results

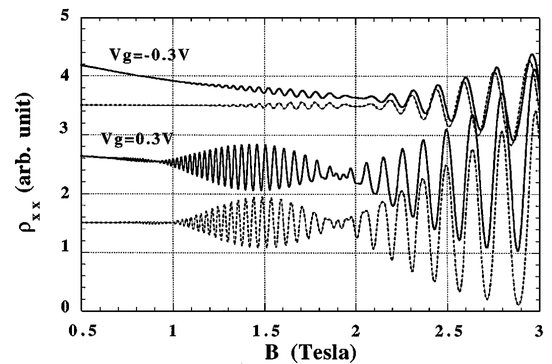

FIG. 4. Comparison between the measured SdH oscillation data and numerical simulations. Solid lines are experimentally measured data; dotted lines are numerical simulations. The parameters used in the calculation are $\Delta_R = 5.6$ meV and $\Gamma = 2.3$ meV for $Vg = -0.3$ V, and $\Delta_R = 5.2$ meV and $\Gamma = 1.4$ meV for $Vg = 0.3$ V.

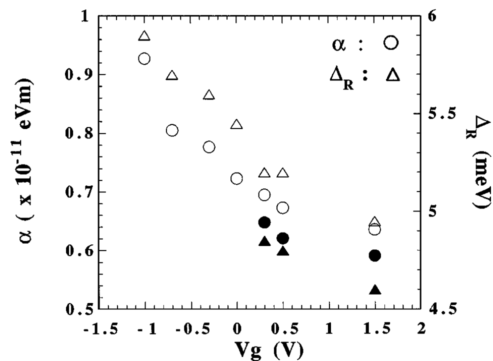

FIG. 5. Gate voltage dependence of the spin-splitting energies Δ_R and the spin-orbit interaction constant α. Circles are the spin-orbit interaction parameters, and triangles are the spin-splitting energy. The open circles and triangles were obtained by fitting the first node positions. The filled symbols were obtained by fitting the second node positions.

supports the Rashba mechanism. The small discrepancy for the second node position and the number of the oscillation of the beat pattern is not yet clear. It will be a future study. We obtained Δ_R by fitting first and second node positions. Then the spin-orbit interaction parameters were calculated using the relation $\Delta_R = 2k_F\alpha$ as a function of the gate voltage Vg.

The gate voltage dependences of Δ_R and α are plotted in Fig. 5. The open circles and triangles were obtained by fitting the first node positions. The filled ones were obtained by the second node positions. As Vg becomes more negative, α and Δ_R are increased. These experimentally obtained α values are the same order as the previously obtained values of 0.9×10^{-11} eV m in an InAs/GaSb quantum well [9], 0.4×10^{-11} eV m in InGaAs/InAlAs systems [10], and 0.6×10^{-11} eV m in an InAs/AlSb quantum well [11]. The increase in α can be attributed to the increase in $\langle E \rangle$ by the negative gate voltage because Vg cannot significantly change m^* and Eg; therefore, the coefficient b can be treated as a constant. We can rule out the mechanism based on the host crystal field. The Rashba term is the only mechanism which can explain the gate voltage dependence because the negative gate voltage enhances the spin-orbit interaction. The spin-orbit interaction parameter α at $Vg = -1$ V is about 1.5 times larger than the value at $Vg = +1.5$ V.

Relating this result to the field effect spin transistor, the spin precession angle $\Delta\theta$ is given by [1]

$$\Delta\theta = 2m^*\alpha L/\hbar^2, \qquad (6)$$

where L is the length between injector and collector ferromagnetic electrodes. This implies that the spin precession angle which is proportional to α can be controlled by the gate voltage Vg. If we assume $L = 0.4\ \mu$m, the spin precession angle can be controlled from $\Delta\theta = \pi$ at $Vg = 1.5$ V to $\Delta\theta = 1.5\pi$ at $Vg = -1$ V. To get a maximum current modulation, it is necessary to control from $\Delta\theta = \pi$ to $\Delta\theta = 2\pi$. In this experiment, α did not reach a saturated value in the above gate voltage range. It will be possible to improve the gate insulation properties and get larger α modulation.

In conclusion, the spin-orbit interaction parameter α in an inverted $In_{0.53}Ga_{0.47}As/In_{0.52}Al_{0.48}As$ heterostructure with a gate-fitted structure has been studied from the viewpoint of device application which has been proposed by Datta and Das [1]. We have experimentally demonstrated that α can be controlled by the interface electric field because the Rashba mechanism is dominant. This result suggests that the precession of the injected polarized spin can be controlled by the gate voltage. This is the first step for realizing the spin-polarized field effect transistor.

We thank Dr. V. Antonov for his help in making the measurement program. We are also indebted to Dr. T. Ikegami, Dr. N. Matsumoto, and Dr. Y. Ishii for their encouragement.

[1] S. Datta and B. Das, Appl. Phys. Lett. **56**, 665 (1989).
[2] R. Eppenga and M. F. H. Schuurmans, Phys. Rev. B **37**, 10 923 (1988).
[3] H. Riechert, S. F. Alvarado, A. N. Tikov, and I. Safarov, Phys. Rev. Lett. **52**, 2297 (1984).
[4] N. E. Christensen and M. Cardona, Solid State Commun. **51**, 491 (1984).
[5] P. D. Dresslhaus, C. M. A. Papavassiliou, R. G. Wheeler, and R. N. Sacks, Phys. Rev. Lett. **68**, 106 (1992).
[6] E. I. Rashba, Fiz. Tverd. Tela (Leningrad) **2**, 1224 (1960) [Sov. Phys. Solid State **2**, 1109 (1960)].
[7] Y. A. Bychov and E. I. Rashba, J. Phys. C **17**, 6039 (1984).
[8] G. Lommer, F. Malcher, and U. Rössler, Phys. Rev. Lett. **60**, 728 (1988).
[9] J. Luo, H. Munekata, F. F. Fang, and P. J. Stiles, Phys. Rev. B **38**, 10 142 (1988); Phys. Rev. B **41**, 7685 (1990).
[10] B. Das, D. C. Miller, S. Datta, R. Reifenberger, W. P. Hong, P. K. Bhattacharya, J. Singh, and M. Jaffe, Phys. Rev. B **39**, 1411 (1989).
[11] J. P. Heida, B. J. van Wees, T. M. Klapwijk, and G. Borghs, in *Proceedings of the 23rd International Conference on the Physics of Semiconductors* edited by M. Scheffler and R. Zimmermann (World Scientific, Singapore, 1996) Vol. 3, p. 2467.
[12] T. Akazaki, T. Enoki, K. Arai, and Y. Ishii, Solid State Electron **38**, 997 (1995).
[13] T. Akazaki, J. Nitta, H. Takayanagi, T. Enoki, and K. Arai, J. Electron. Mater. **25**, 745 (1996).